

⁷ Hayes, W. D. and Probstein, R. F., *Hypersonic Flow Theory*, Academic Press, New York, 1959.

⁸ Davis, R. T., "Numerical Solution of the Hypersonic Viscous Shock-Layer Equations," *AIAA Journal*, Vol. 8, No. 5, May 1970, pp. 843-851.

⁹ Stewartson, K., "On the Motion of a Flat Plate at High Speed in a Viscous Compressible Fluid—II Steady Motion," *Journal of the Aeronautical Sciences*, Vol. 22, No. 5, 1955, pp. 303-309.

¹⁰ Bertram, M. H. and Blackstock, T. A., "Some Simple Solutions to the Problem of Predicting Boundary-Layer Self Induced Pressures," TN D-798, April 1961, NASA.

¹¹ Feldhuhn, R. H., "An Experimental Investigation of the Effects of Leading Edge Reynolds Number and Angle of Attack of the Flow of Helium Over a Flat Plate at $M = 16.35$," Internal Memo. 8, July 1965, Dept. of Aerospace and Mechanical Sciences, Gas Dynamics Lab., Princeton Univ., Princeton, N. J.

¹² Hall, J. G. and Golian, T. C., "Shock Tunnel Studies of Hypersonic Flat Plate Air Flow," Rept. AD-1052-A-10, 1960, Cornell Aerospace Lab., Buffalo, N. Y.

¹³ Cheng, H. K., Hall, J. G., Golian, T. C., and Hertzberg, A., "Boundary Layer Displacement and Leading-Edge Bluntness Effects in High Temperature Hypersonic Flow," *Journal of the Aerospace Sciences*, Vol. 28, No. 5, 1961, pp. 353-381.

Molecular Beam Extraction from Equilibrium Gas Flows

ULF BOSSEL*

DFVLR-AVA, Göttingen, West Germany

Theory

CONSIDER the beam system schematic, Fig. 1. If density-sensitive detectors are used, as in the present case, then the beam properties are found as the moments of the distribution describing the state of the gas inside the beam source region from which the beam molecules are isolated. For flux-sensitive devices the detection signal should be proportional to the moments of the distribution function augmented factorially by a detection, or plane crossing probability ($\mathbf{c} \cdot \mathbf{v}$), the scalar product of the molecular velocity \mathbf{c} and the plane normal \mathbf{v} . Here the concept of an escape probability associated with beam formation in conventional studies has been generalized to a plane-crossing probability associated with particular de-

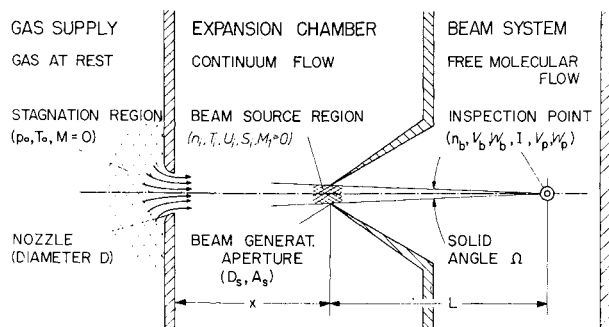


Fig. 1 Schematic of beam generation system.

Received June 18, 1970; revision received June 8, 1971. Experiments carried out at the University of California, Berkeley, Calif., and numerical work conducted at Syracuse University were combined at Göttingen. The author gratefully acknowledges support of all three institutions.

Index categories: Rarefied Flows; Supersonic and Hypersonic Flow; Atomic, Molecular, and Plasma Properties.

* Research Scientist, Department of Space Aerodynamics.

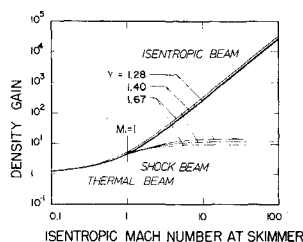


Fig. 2 Density gain vs isentropic skimmer Mach number.

tection techniques. The results of the obvious integrations over small solid angles $0 < \Omega \equiv A_s/L^2 \ll 4\pi$ are listed in Table 1, since no comprehensive tabulation can be found elsewhere.

Skimming Models

Two extreme cases are considered for the isolation of nozzle beams from equilibrium gas flows. The isentropic model¹ neglects interference of the skimmer with the incoming flow. The beam source conditions, index 1, are related to the stagnation region via the isentropic expansion laws. If the flow is completely randomized prior to beam formation by either a normal shock ahead of, or at the skimmer, or by diffuse adiabatic scattering inside the skimmer, then the isentropic laws are augmented by the Rankine-Hugoniot relations. The shock-beam² properties therefore deserve the index 2. Consequently, the density n_i , temperature T_i and molecular speed ratio S_i in Table 1 must be replaced by the appropriate beam source conditions depending on the case considered.

Figures 2 and 3 illustrate the nature of shock beams. They are neither supersonic, nor effusive, but could be classified as subsonic nonisentropic beams. Figure 2 shows that such beams are denser than effusive reference beams from a thermal source at isentropic freestream density n_1 . Naturally, they are less dense than isentropic supersonic beams because of the partial loss of precollimation during the shock transition. The significance of the branchpoint at $M_1 = 1$ is obvious. The shock beam formation requires $M_1 \geq 1$.

Similarly, Fig. 3 reveals that the average velocity V_b of diatomic shock beam molecules is between that of an effusive and an isentropic supersonic beam. Whereas $V_{b,1}$ and the isentropic drift U_1 merge at higher skimmer Mach numbers M_1 , $V_{b,2}$ remains significantly greater than U_2 indicating that effusive phenomena dominate in the shock beam formation.

Experimental Results

The experimental setup has been described elsewhere.³ Only the near-inviscid portion ($8000 < Re^* \equiv \rho^* Da^* / \mu^* < 50,000$) of the slender 0.027 cm skimmer data are checked against theory. The observed beam density data are presented in Fig. 4 as a function of the computed total number flux \dot{N}_{tot} into the skimmer and the stagnation pressure p_0 . We wish to demonstrate that the outer maxima near D relate

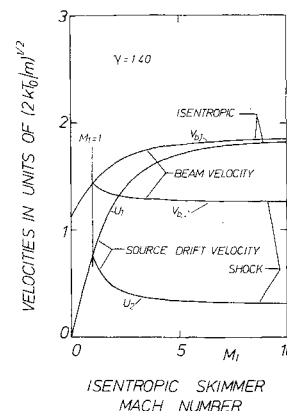


Fig. 3 Comparison of beam and source drift velocities.

Table 1 Ideal properties of molecular beam skimmed from parallel equilibrium gas flows

Distribution inside beam source region: $f_i(c) = n_i(2\pi kT_i/m)^{-3/2} \exp[-m(c - U_i) \cdot (c - U_i)/(2kT_i)]$		
	density-sensitive beam detection	flux-sensitive beam detection
beam detection distribution	$f_i(c)$	$g_i(c) = (c \cdot U_i)f_i(c)$
density/intensity	$n_{b,i} = n_i\Omega/(4\pi)D(S_i)$	$I_i = n_i\Omega/(4\pi)[8kT_i/(\pi m)]^{1/2}F(S_i)$
profiles along circular arc, radius L , centered at skimmer	$n_{b,i}(\theta) = n_i\Omega/(4\pi) \cos\theta \times D(S_i \cos\theta) \exp[-(S_i \sin\theta)^2]$	$I_i(\theta) = n_i\Omega/(4\pi)[8kT_i/(\pi m)]^{1/2} \cos\theta \times F(S_i \cos\theta) \exp[-(S_i \sin\theta)^2]$
gain	$\text{GAIN}_{n,i} = (n_i/n_i)D(S_i)$	$\text{GAIN}_{I,i} = (n_i/n_i)(T_i/T_0)^{1/2}F(S_i)$
most probable speed of beam molecules (b.m.)	$C_{b,i} = [2kT_i/m]^{1/2} [(1 + S_i^2/4)^{1/2} + S_i/2]$	$C_{p,i} = [3kT_i/m]^{1/2} [(1 + S_i^2/6)^{1/2} + (S_i^2/6)^{1/2}]$
mean speed of b.m.	$V_{b,i} = [8kT_i/(\pi m)]^{1/2} F(S_i)/D(S_i)$	$V_{p,i} = [9\pi kT_i/(8m)]^{1/2} E(S_i)/F(S_i)$
r.m.s. speed of b.m.	$W_{b,i} = [3kT_i/m]^{1/2} [E(S_i)/D(S_i)]^{1/2}$	$W_{p,i} = [4kT_i/m]^{1/2} [Q(S_i)/F(S_i)]^{1/2}$
mean kinetic energy of b.m. with the abbreviations	$e_{b,i} = (3/2)kT_i E(S_i)/D(S_i)$ $D(X) = 2\pi^{-1/2}Xa + (2X^2 + 1)b$ $F(X) = (X^2 + 1)a + \pi^{1/2}(X^3 + \frac{3}{2}X)b$ $E(X) = \pi^{-1/2}(\frac{4}{3}X^3 + \frac{10}{3}X)a + (\frac{4}{3}X^4 + 4X^2 + 1)b$ $Q(X) = (\frac{1}{2}X^4 + \frac{9}{4}X^2 + 1)a + \pi^{1/2}(\frac{1}{2}X^5 + \frac{5}{2}X^3 + \frac{3}{8}X)b$	$e_{p,i} = 2kT_i Q(S_i)/F(S_i)$

and $a = \exp(-X^2)$, $b = 1 + \text{erf}(X)$, $S_i = U_i(2kT_i/m)^{-1/2} = M_i(\gamma/2)^{1/2}$, $\Omega = A_s/L^2$

The angle θ is measured from the beam axis.

to isentropic beams, whereas the maxima at A are the remainders of shock beams heavily attenuated by scattering.

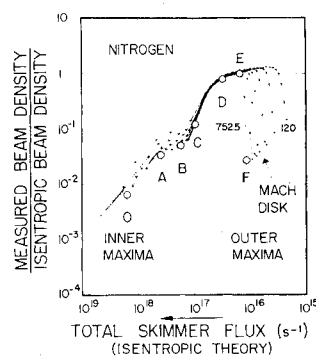
Figure 5 relates the observed to the predicted isentropic beam density. The curves collapse near the outer maxima at D and also near unity, i.e., theory and experiment agree up to a constant factor. This normalization fails to produce any correlation in the shock beam range.

In Fig. 6 the observations are compared to the shock beam theory. Experiment and analysis coincide near the inner maximum at A. Also, a relative density near unity is obtained at the optima, indicating that the shock beam model yields an excellent description of the perturbed process of beam formation at least for the present set of experiments.

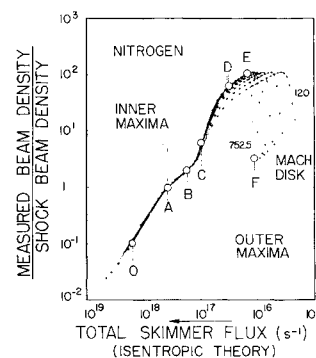
The striking coalescence of the seven traces at either maximum and the correlation between theory and experiment at the point of coalescence seem to support the presented augmentation of the Kantrowitz-Grey-Parker⁴ theory. One would have expected the maxima to occur at a $1/e$ attenuation. Also, in the free molecule limit, $\dot{N}_{\text{tot}} \rightarrow 0$, the upper envelope in Fig. 5 should approach unity. These discrepancies are of similar magnitude at the three significant points here considered. This strongly suggests that a systematic error has entered the experiments.

Discussion

The model for the formation of shock beams is consistent with the experimental results of Bier and Hagen.⁵ Certainly, re-expansion downstream of the compression region may be present, but the dominating phenomenon appears to be effusion from a beam source region which itself is moving at the subsonic velocity U_2 . Also, the proposed shock beam model does not conflict with the results of electron beam studies by McMichael and French⁶ since bow shock formation is restricted to denser flows than studied at Toronto. On the

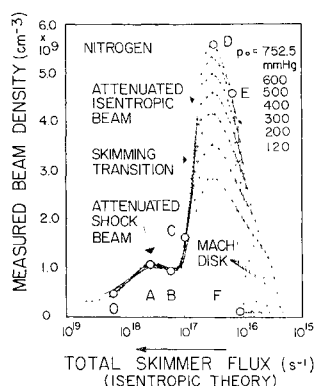
Fig. 5 Beam density compared to isentropic-beam theory.

other hand, Oman⁷ has shown that the observed⁸ small density perturbation near the skimmer lip trigger the build-up of the molecular population within the skimmer duct which leads to the formation of shock beams. As far as the use of nozzle beams for diagnostic purposes is concerned, the regions behind or within normal shocks appear to be no longer off-limits for molecular beam sampling, if the observations are related to analyses which incorporate the shock beam model in its proposed or in a modified form.

Fig. 6 Beam density compared to shock-beam theory.

References

- Kantrowitz, A. and Grey, J., "A High Intensity Source for the Molecular Beam. Part I: Theoretical," *Revue of Scientific Instruments*, Vol. 22, May 1951, pp. 328-332.
- Bossel, U., "Skimmer Interaction: Transition from a "Shock Beam" to a Supersonic Nozzle Beam," *Entropie*, No. 30, Nov.-Dec. 1969, pp. 11-15.
- Bossel, U., Hurlbut, F. C., and Sherman, F. S., "Extraction of Molecular Beams from Nearly-Inviscid Hypersonic Free Jets," *Proceedings of the Sixth International Symposium on Rarefied Gas Dynamics*, Vol. 2, Academic Press, New York, 1969, pp. 945-964.

Fig. 4 Beam density vs total skimmer flux.

⁴ Parker, H. M., Kuhlthau, A. R., Zapata, R., and Scott, J. E., "The Application of Supersonic Beam Source to Low-Density High-Velocity Experimentation," *Proceedings of the First International Symposium on Rarefied Gas Dynamics*, Pergamon Press, New York, 1960, pp. 69-79.

⁵ Bier, K. and Hagen, O. F., "Influence of Shock Waves on the Generation of High-Intensity Molecular Beams by Nozzles," *Proceedings of the Third International Symposium on Rarefied Gas Dynamics*, Vol. 1, Academic Press, New York, 1963, pp. 478-496.

⁶ McMichael, G. E. and French, J. B., "Electron-Beam Studies of Skimmer Interaction in a Free Jet," *The Physics of Fluids*, Vol. 9, July 1966, pp. 1419-1420.

⁷ Oman, R. A., "Analysis of a Skimmer for a High-Intensity Molecular Beam Using a Three-Fluid Model," *The Physics of Fluids*, Vol. 6, July 1963, p. 1031.

⁸ French, J. B. and McMichael, G. F., "Progress in Developing High Energy Nozzle Beams," *Proceedings of the Fifth International Symposium on Rarefied Gas Dynamics*, Vol. 2, Academic Press, New York, 1967, pp. 1385-1392.

Stability of Transient Solution of Moderately Thick Plate by Finite-Difference Method

TIEN YU TSUI*

Army Materials and Mechanics Research Center,
Watertown, Mass.

AND

PIN TONG†

Massachusetts Institute of Technology,
Cambridge, Mass.

Introduction

THE finite-difference method, widely used in the solution of the equation of motion which governs the transient response of structures such as plates and shells, can become unstable unless the ratio of the time mesh to the space mesh satisfies a certain condition. The condition of stability of the finite-difference equation for the transient response of a "thin" flat plate has been given by Leech.¹ This paper is concerned with the same problem for a "moderately thick" plate. The method of stability analysis used here follows that employed in Ref. 1.

Method of Analysis

The governing equation of motion of a moderately thick plate has been derived by Mindlin² as follows:

$$\left(\nabla^2 - \frac{\rho}{G'} \frac{\partial^2}{\partial t^2}\right) \left(D \nabla^2 - \frac{\rho h^3}{12} \frac{\partial^2}{\partial t^2}\right) w + \rho h \frac{\partial^2 w}{\partial t^2} = 0 \quad (1)$$

where w is the displacement normal to the initial plane of the plate, D the flexural rigidity of the plate, ρ the density of plate material, h the plate thickness, and G' is related to the shear modulus G by $G' = (\pi^2/12)G$. The preceding equation includes the effect of rotatory inertia and transverse shear. When a square space mesh $\Delta x = \Delta y$ is used the corresponding explicit finite-difference equation for Eq. (1) may be written

as follows:

$$\begin{aligned} [D/(\Delta x)^4] & (w_{j-2,k} - 8w_{j-1,k} + 20w_{j,k} - 8w_{j+1,k} + \\ & w_{j+2,k} + 2w_{j-1,k+1} - 8w_{j,k+1} + 2w_{j+1,k+1} + \\ & w_{j,k+2} + 2w_{j-1,k-1} - 8w_{j,k-1} + 2w_{j+1,k-1} + \\ & w_{j,k-2})_n - [a/(\Delta x \Delta t)^2] [(w_{j+1,k} - 4w_{j,k} + \\ & w_{j-1,k} + w_{j,k+1} + w_{j,k-1})_{n+1} - 2(w_{j+1,k} - \\ & 4w_{j,k} + w_{j-1,k} + w_{j,k+1} + w_{j,k-1})_{n-1} + \\ & (w_{j+1,k} - 4w_{j,k} + w_{j-1,k} + w_{j,k+1} + w_{j,k-1})_{n-1}] + \\ & [b/(\Delta t)^4] (w_{n+2} - 4w_{n+1} + 6w_n - 4w_{n-1} + \\ & w_{n-2})_{j,k} + [c/(\Delta t)^2] (w_{n+1} - 2w_n + w_{n-1})_{j,k} = 0 \quad (2) \end{aligned}$$

where $a = \rho h^3/12 \times D\rho/G'$, $b = \rho^2 h^3/12G'$, $c = \rho h$. In Eq. (2) j and k denote space mesh stations x and y , respectively, and n denotes the current time t . When the value of w has been determined at all space mesh points for the last two time increments n and $n-1$, one can directly calculate the solution for the next time increment $n+1$ from Eq. (2), thus advancing the solution in time. The first two values required to start the whole numerical process are obtained from the initial conditions. If it is assumed in the practical solution of the finite-difference Eq. (2) that the error $\delta(x,y,t)$ is resulted from roundoff, it must satisfy the following equation:

$$\begin{aligned} [D/(\Delta x)^4] & (\delta_{j-2,k} - 8\delta_{j-1,k} + 20\delta_{j,k} - 8\delta_{j+1,k} + \\ & \delta_{j+2,k} + 2\delta_{j-1,k+1} - 8\delta_{j,k+1} + 2\delta_{j+1,k+1} + \\ & \delta_{j,k+2} + 2\delta_{j-1,k-1} - 8\delta_{j,k-1} + 2\delta_{j+1,k-1} + \\ & \delta_{j,k-2})_n - [a/(\Delta x \Delta t)^2] [(\delta_{j+1,k} - 4\delta_{j,k} + \\ & \delta_{j-1,k} - \delta_{j,k+1} + \delta_{j,k-1})_{n+1} - 2(\delta_{j+1,k} - \\ & 4\delta_{j,k} + \delta_{j-1,k} + \delta_{j,k+1} + \delta_{j,k-1})_{n-1} + (\delta_{j+1,k} - \\ & 4\delta_{j,k} + \delta_{j-1,k} + \delta_{j,k+1} + \delta_{j,k-1})_{n-1}] + \\ & [b/(\Delta t)^4] [\delta_{n+2} - 4\delta_{n+1} + 6\delta_n - 4\delta_{n-1} + \\ & \delta_{n-2})_{j,k} + [c/(\Delta t)^2] (\delta_{n+1} - 2\delta_n + \delta_{n-1})_{j,k} = 0 \quad (3) \end{aligned}$$

Following the procedure employed by Leech,¹ it is assumed that the general term of the Fourier series expansion of the numerical error may be expressed in the form

$$\delta_{j,k,n} = e^{\alpha n \Delta t} e^{i\beta j \Delta x} e^{i\gamma k \Delta y} \quad (4)$$

Making use of Eqs. (3) and (4) one obtains the following equation:

$$\begin{aligned} \left[(\xi)^{1/2} - \frac{1}{(\xi)^{1/2}} \right]^4 + r^2 \left[4 \left(\frac{a}{b} \right) \left(\sin^2 \frac{\beta \Delta x}{2} + \sin^2 \frac{\gamma \Delta y}{2} \right) + \right. \\ \left. \left(\frac{c}{b} \right) (\Delta x)^2 \right] \left[(\xi)^{1/2} - \frac{1}{(\xi)^{1/2}} \right]^2 + \\ \frac{16Dr^4}{b} \left(\sin^2 \frac{\beta \Delta x}{2} + \sin^2 \frac{\gamma \Delta y}{2} \right)^2 = 0 \quad (5) \end{aligned}$$

where $\xi = e^{\alpha \Delta t}$ and $r = \Delta t/\Delta x$. For convenience in examining the stability of the finite-difference solution, the following symbol is introduced:

$$Z = \left[(\xi)^{1/2} - \frac{1}{(\xi)^{1/2}} \right]^2 \quad (6)$$

In terms of Z , Eq. (5) becomes

$$Z^2 + 2r^2 \alpha Z + r^4 \beta = 0 \quad (7)$$

where

$$\begin{aligned} \alpha &= 2(a/b) [\sin^2(\beta \Delta x/2) + \sin^2(\gamma \Delta y/2)] + (c/2b) (\Delta x)^2 \\ \beta &= (16D/b) [\sin^2(\beta \Delta x/2) + \sin^2(\gamma \Delta y/2)]^2 \end{aligned}$$

Received February 22, 1971; revision received April 26, 1971.

* Mechanical Engineer, Structural Mechanics Division, Theoretical and Applied Mechanics Research Laboratory.

† Associate Professor, Department of Aeronautics and Astronautics.